

LRP 357/88

October 1988

ION TEMPERATURE MEASUREMENTS OF A TOKAMAK  
PLASMA BY COLLECTIVE THOMSON SCATTERING OF  
D<sub>2</sub>O LASER RADIATION

R. Behn, D. Dicken, J. Hackmann, S.A. Salito &  
M.R. Siegrist

ION TEMPERATURE MEASUREMENT OF A TOKAMAK PLASMA BY  
COLLECTIVE THOMSON SCATTERING OF D<sub>2</sub>O LASER RADIATION

R. Behn, D. Dicken\*, J. Hackmann\*, S.A. Salito, M.R. Siegrist

Centre de Recherches en Physique des Plasmas

Association Euratom - Confédération Suisse

Ecole Polytechnique Fédérale de Lausanne

21, Av. des Bains - 1007 Lausanne - Switzerland

\* Permanent Address : Institut für Laser- und Plasmaphysik,  
Universität Düsseldorf, FRG

**Abstract** - A D<sub>2</sub>O FIR laser emitting 0.5J in 1.4μs at 385μm and a heterodyne receiver system comprising a Schottky barrier diode mixer with a noise temperature of 8000°K (DSB) were used in a Thomson scattering experiment to measure the ion temperature of a tokamak plasma during a single laser shot. Series of measurements under reproducible plasma conditions have been carried out in H, D and He-plasmas. Their statistical analysis yielded a typical relative error of 25% for a single shot measurement.

## INTRODUCTION

In a tokamak plasma, the ion temperature is an important parameter and considerable efforts have been made to develop methods which can provide measurements with good temporal and spatial resolution. For measurements of the electron temperature these requirements are fulfilled by Thomson scattering using either a ruby or Nd:YAG laser and this method has become a standard of tokamak diagnostics.<sup>1</sup> Thomson scattering from thermal density fluctuations has also been proposed as a method to measure the ion temperature.<sup>2</sup> For a suitable choice of laser wavelength and scattering angle the width of the scattered light spectrum is determined by the ion temperature. In this case the spectrum reflects the collective motion of the electrons forming a shielding cloud which follows the thermal motion of the ions. These conditions are fulfilled when the parameter  $\alpha = 1/|k| \cdot \lambda_D$  ( $k$ =difference wave vector,  $\lambda_D$ =Debye length) is larger than 1.

For typical tokamak parameters and scattering angles permitting good spatial resolution, a laser source in the far infrared is required. When selecting a particular laser system for a  $T_i$  measurement several points have to be considered:

- 1) The capability of the laser of high power and long pulse operation;
- 2) The sensitivity and bandwidth of the detectors available;
- 3) The plasma radiation level (e.g. electron cyclotron emission).

This has led to the choice of the optically pumped D<sub>2</sub>O laser with its stimulated Raman transition at 385  $\mu$ m. At this wavelength Schottky barrier diode mixers allow heterodyne detection with an NEP down to  $10^{-19}$  W/Hz and an IF bandwidth in the GHz range. Long pulse operation of the laser is important, because it will determine the signal integration time which finally limits the

signal-to-noise ratio that can be achieved.<sup>3,4</sup>

After several years of development of powerful FIR lasers and sensitive detection systems, the first results from collective Thomson scattering using a pulsed D<sub>2</sub>O laser were reported in 1983 by Woskoboinikow et al.<sup>5</sup> However, because of severe stray light problems and limited signal-to-noise ratio, an ion temperature measurement was not feasible at that time.

In the following results from an experiment on the TCA tokamak will be presented, permitting for the first time to evaluate the ion temperature from the data obtained during a single laser shot.

## EXPERIMENT

The experimental set-up is shown schematically in Fig. 1. The main components are the D<sub>2</sub>O laser resonator, a high power CO<sub>2</sub> laser for optical pumping and a heterodyne receiver system with 12 spectral channels. The CO<sub>2</sub> laser system consists of a hybrid-TEA laser oscillator tuned to the 9R(22) line followed by an e-beam preionized amplifier in a triple-pass configuration. Under typical operating conditions the laser delivers 600J in a 1.4 $\mu$ s single-mode pulse.<sup>6</sup> A 70m long beam duct comprising several mirrors was necessary because space limitations excluded the installation of the CO<sub>2</sub> laser next to the FIR laser in the experimental hall of the TCA tokamak. For the 9R(22) laser line there is very little absorption in dry air, so that evacuation or special gas filling of the beam duct was not necessary. At present, the maximum pump power that can be used is limited by the damage threshold of the input window of the D<sub>2</sub>O laser vessel rather than by the CO<sub>2</sub> laser itself. The D<sub>2</sub>O laser has a 4m long unstable resonator in L-shape with a wire grid at the vertex to allow efficient coupling of the pump beam. At a

filling pressure of 6.5mbar the FIR laser produces 0.5J in 1.4 $\mu$ s.

The D<sub>2</sub>O laser emission is focused to a 3mm waist close to the plasma centre via a set of off-axis parabolic mirrors. A conical pyrex beam dump is used to absorb the laser beam and a deeply grooved Macor ceramic viewing dump is attached to the tokamak vessel opposite to the output window. The purpose of these two devices is to reduce stray light to an acceptable level. The scattered light is collected at 90° to the incident beam in a solid angle of  $4.3 \cdot 10^{-3}$  sterad. A combination of mirrors is used to image the scattering volume onto the detector. Since the beam path to the receiver system is about 10m, absorption in air (rel. humidity around 50%) would cause noticeable losses. Therefore the largest part of the trajectory (7m) is inside a beam duct filled with dry nitrogen.

For detection and spectral analysis of the scattered radiation we use a heterodyne receiver with an optically-pumped CD<sub>3</sub>Cl FIR laser as local oscillator. Its emission is combined with the scattered radiation in an optical diplexer and mixed in a Schottky barrier diode. The resulting IF signal, centered around 3.6 GHz, is amplified and split into 12 channels. The channels with a bandwidth of 80MHz each have been chosen to cover the part of the scattered light spectrum shifted from the laser line towards higher frequencies. The signals from the output of the receiver are fed into a CAMAC-ADC which comprises a gated integrator. After each shot the data from the internal buffer memory are transferred to the local computer via fiber optic links.

The collaboration with groups at the University of Duesseldorf and the MPI fuer Radioastronomie, Bonn (FRG), resulted in a considerable improvement of the sensitivity of our detection system. The essential step was a replacement of the Schottky diode mixer and the first IF amplifier. Calibration of the receiver using

black-body sources yielded a system noise temperature of  $8000^{\circ}$  K (DSB), equivalent to a NEP of  $2.2 \cdot 10^{-19}$  W/Hz. A summary of the essential parameters of our experimental set-up is given in Table I.

Typical pulses of the CO<sub>2</sub> and the D<sub>2</sub>O laser, recorded by fast detectors, are shown in Fig. 2. The beating of 2 to 3 modes is observed in the FIR signal. This corresponds to an emission bandwidth of 100-150 MHz which is compatible with the desired spectral resolution, but can only be achieved with a single mode pump pulse. The gate duration of the ADC, during which the signal is integrated, was adjusted to match the laser pulse length (1.4 $\mu$ s). The acquisition system was set to record also a series of 9 samples during a period of 100 $\mu$ s before and after the laser pulse. From these additional samples we can determine the fluctuations in the signal level caused by background radiation and noise in the receiver system. This information is used to evaluate the error bars for single shot measurements. In our case the background radiation from the plasma can be neglected since the laser frequency is far above the low-order harmonics of the electron cyclotron frequency (40GHz).

## RESULTS

During the experiments on TCA series of measurements for different majority ion species have been carried out. Within each series several shots with reproducible plasma parameters were obtained allowing to average the results to obtain better signal-to-noise ratios. As an exemple Fig. 3 shows the mean value of 10 shots in a H-plasma. The data from 7 reproducible shots in a D-plasma were averaged to obtain the spectrum presented in Fig. 4. It should be pointed out that there is no signal in the absence of a plasma (full circles in Fig. 4), indicating that stray light is negligible in this part of the spectrum. With helium (He) as the

majority ion species the spectrum presented in Fig. 5 is obtained. The change in the width of the spectrum with increasing ion mass can be seen more clearly in Fig. 6 where the data of the 3 previous figures have been superposed. The vertical scale on the graph is arbitrary; the scale factors are determined by the fitting routine from a comparison of the experimental data with the fitted spectrum.

A typical result of a quantitative analysis is given in Fig. 7 where the ion temperature of a hydrogen plasma has been obtained from a single shot measurement. The curve represents the theoretical spectrum obtained from a least-square fitting procedure with the ion temperature as the only free parameter. Other plasma data like the electron density and temperature, the magnetic field and the impurity concentrations are introduced as fixed parameters. The error bars were calculated in the following way: the statistical fluctuations of the noise level were obtained from the series of acquisitions before and after each laser pulse. Signal-to-noise calculations for heterodyne detection permit to determine the increase in the standard deviation due to the presence of a fluctuating signal. This calculation is based on the expectation value of the signal as found by the fitting routine. Therefore the error bars are centered on the theoretical curve rather than the experimental data points.

In Table II we compiled the measured ion temperatures for series of plasma shots with reproducible plasma parameters. The averages and resulting standard deviations of the mean and of a single shot measurement are also given. It should be mentioned that systematic errors caused by uncertainties in the input parameters are not included.

## DISCUSSION

The influence of impurity ions and a magnetic field on the shape of the spectrum can be seen on Fig. 8 showing calculated spectra for a H-plasma. The theoretical model used for these calculations applies to a thermal plasma with several ion species (majority ions and impurities).<sup>7</sup> For a scattering geometry where the difference wave vector  $k=k_s - k_i$  is almost perpendicular to the total magnetic field vector  $B = B_{\text{tor}} + B_{\text{pol}}$  the shape of the spectrum is very sensitive to the angle  $\beta$  between  $k$  and  $B$ .

While the contribution from the impurities is dominating near the center, the magnetic field also influences the shape at larger frequency shifts. However, this effect is almost negligible when the angle  $\beta$  is chosen to be less than  $85^\circ$ . For our present set-up the angle  $\beta$  is about  $89^\circ$ . This value corresponds to our scattering geometry and a typical q-profile of the plasma. We have also taken into account that the scattering volume is located at about 1cm from the magnetic axis and that averaging over the solid angle of observation leads to an increase in the effective angle.

Since there is a remaining uncertainty about this parameter which affects the  $T_i$  value found by the fitting procedure, we will change the scattering geometry in future experiments to avoid this strong influence of the magnetic field. Although our fitting routine includes the impurity contributions which predominantly influence the centre of the spectrum, we have excluded a 400 MHz band, starting at the laser line, from the data analysis. At present, we do not have sufficient information about local concentrations of the impurity species in TCA. Furthermore, stray light contributes to the signal in 2 to 3 channels next to the laser line and as a result the data in the central channels would be difficult to



interpret. As long as the main interest is in the temperature of the majority ions, it is essential to resolve the wings of the spectrum, where the influence of impurity ions and stray light can be neglected.

## SUMMARY

Measurements of the ion temperatures of tokamak plasmas with different majority ion species (H, D, and He) are presented. The ion temperatures were obtained by collective Thomson scattering from thermal density fluctuations. The experimental set-up at the TCA tokamak comprises an optically pumped D<sub>2</sub>O laser emitting at 385 $\mu$ m and a 12-channel heterodyne receiver system. The FIR laser produces 0.5J in a 1.4 $\mu$ s pulse. For the heterodyne receiver, which includes a Schottky barrier diode mixer, a system noise temperature of 8000° K (DSB) has been obtained. At high plasma densities the signal-to-noise ratios were sufficient for measurements of the ion temperature during a single laser shot.

## ACKNOWLEDGEMENT

The authors are indebted to P.A. Krug and I. Kjelberg for their collaboration during the system development, to H.P. Roeser for supplying the Schottky diode mixer and to the tokamak operators for many hours of machine time. The expert technical assistance of G. Bochy was also greatly appreciated.

## REFERENCES

- 1 N.C. Luhmann, W.A. Peebles  
Instrumentation for magnetically confined fusion plasma diagnostics  
Rev. Sci. Instr. **55**(3), 279 - 331 (1984)
- 2 D.E. Evans  
Thomson scattering of FIR radiation  
UKAEA Culham Laboratory Report CLM-P 482, 1977

- 3 L.E. Sharp, A.D. Sanderson, D.E. Evans  
Signal-to-noise requirements for interpreting submillimeter laser scattering experiments in a tokamak plasma  
Plasma Phys. **23**(4), 357 - 370 (1981);
- 4 R.L. Watterson, M.R. Siegrist, M.A. Dupertuis, P.D. Morgan, M.R. Green  
Numerical simulation of a system for ion temperature measurement by Thomson scattering in a tokamak  
J. Appl. Phys. **52**, 3249 - 3254 (1981)
- 5 P. Woskoboinikow, W.J. Mulligan, J. Machuzak, D.R. Cohn, R.J. Temkin, T.C.L.G. Sollner, B. Lax  
385 $\mu$ m D<sub>2</sub>O laser collective Thomson scattering ion temperature diagnostic  
11th European Conf. on Contr. Fusion and Plasma Physics, Aachen, FRG, 5 - 9 Sept. 1983
- 6 R. Behn, M.A. Dupertuis, I. Kjellberg, P.A. Krug, S.A. Salito, M.R. Siegrist  
Buffer gases to increase the efficiency of an optically pumped far infrared D<sub>2</sub>O laser  
IEEE J. of Quantum Electronics, **QE-21**, 1278 - 1285 (1985)
- 7 D.E. Evans  
The effect of impurities on the spectrum of laser light scattered by a plasma  
Plasma Phys. **12**, 573 - 584 (1970)

## FIGURE CAPTIONS

- Fig.1 Configuration of the experimental system :
- LO : Hybrid TEA CO<sub>2</sub> laser oscillator
  - TPA : Triple pass CO<sub>2</sub> laser amplifier, e-beam pre-ionized
  - BD : beam duct, 70m long
  - FIRL : D<sub>2</sub>O FIR laser
  - BFO : beam focusing optics
  - TCA : TCA tokamak
  - DP1 : Viewing dump MACOR ceramic
  - DP2 : Beam dump PYREX cone
  - BCO : Beam collection optics with 7m long dry nitrogen filled beam duct
  - D : Diplexer
  - LOL : Local oscillator laser
  - SDM : Schottky diode mixer
  - HRS : Heterodyne receiver system
- Fig. 2 Typical pump and far-infrared laser pulses
- Fig. 3 H-spectrum obtained by averaging 10 shots with reproducible plasma parameters.
- Fig. 4 D-spectrum obtained by averaging 7 shots with reproducible plasma parameters. Full circles : without plasma
- Fig. 5 He-spectrum obtained by averaging 9 shots with reproducible plasma parameters

Fig. 6 Superposition of the spectra presented in Figs. 3 - 5

Fig. 7 Single shot measurement in a H-plasma

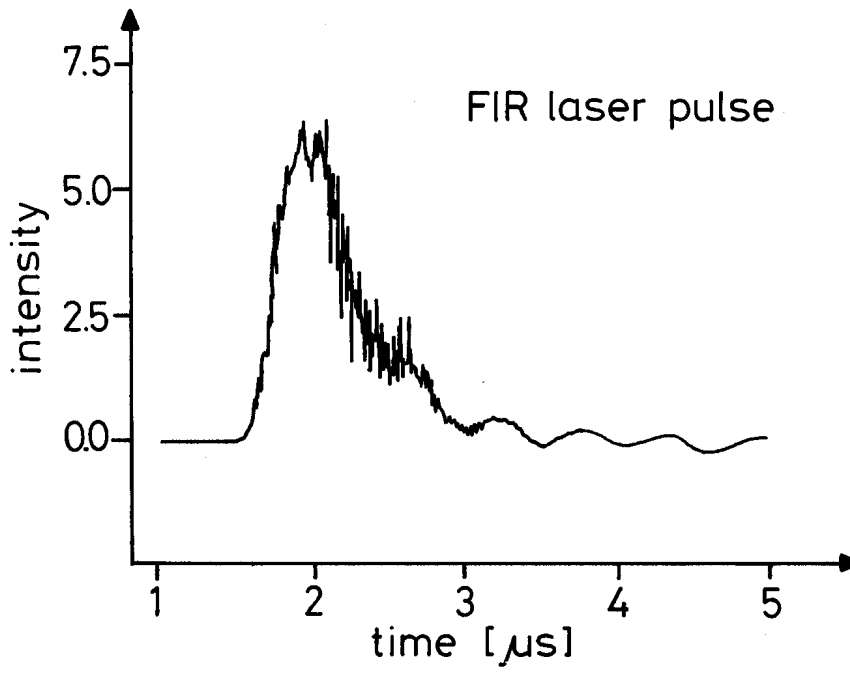
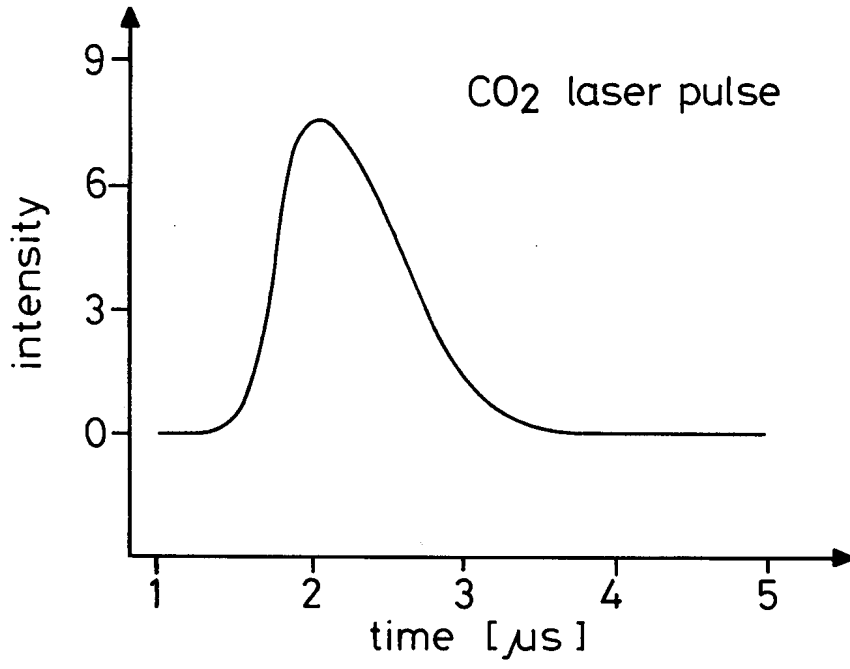
Fig. 8 Calculated spectra for a H-plasma  
 (1) no impurities, no magnetic field  
 (2) impurities included (C, O, Fe;  $Z_{\text{eff}} = 2.5$ ); no magnetic field  
 (3) no impurities; magnetic field at  $89^\circ$   
 (4) impurities included; magnetic field at  $89^\circ$

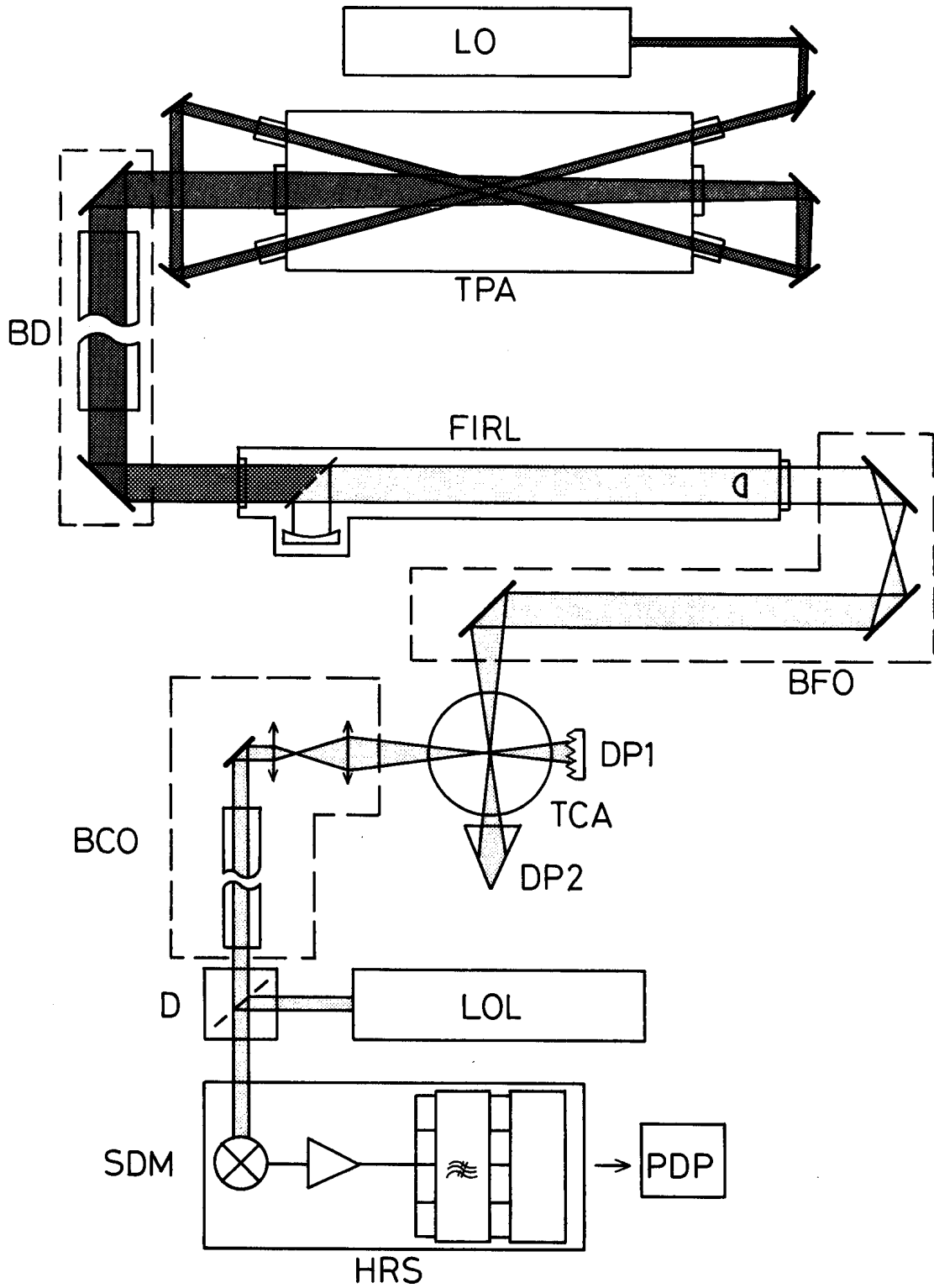
**TABLE I System Parameters**

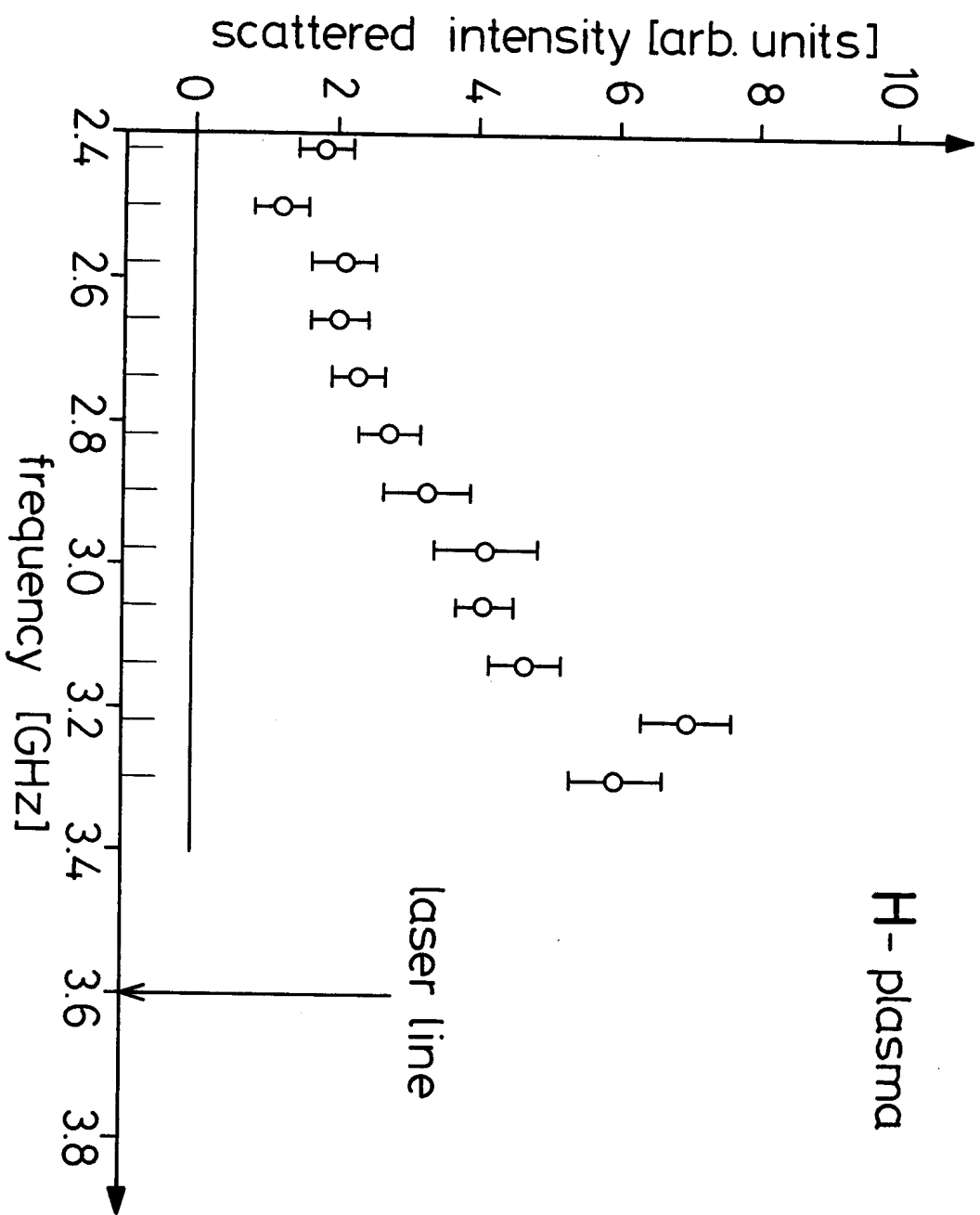
|   |                            |
|---|----------------------------|
| Laser wavelength                                    | 385 $\mu\text{m}$          |
| Laser power   | 400 kW                     |
| Detector BSD noise temperature                      | 8000°K                     |
| Channel center frequencies (relative to laser line) | 300 to 1180 MHz            |
| Channel width                                       | 80 MHz                     |
| Gate duration                                       | 1.4 $\mu\text{s}$          |
| Scattering angle                                    | $90^\circ$                 |
| $\beta$ (k, B)                                      | $89^\circ$                 |
| $\alpha$  | 1.7                        |
| F-number of collecting and focusing lens            | 13.5                       |
| Focal spot radius                                   | 3.3 mm                     |
| Solid angle   | $4.3 \cdot 10^{-3}$ sterad |

**TABLE II Summary of  $T_i$  measurements**

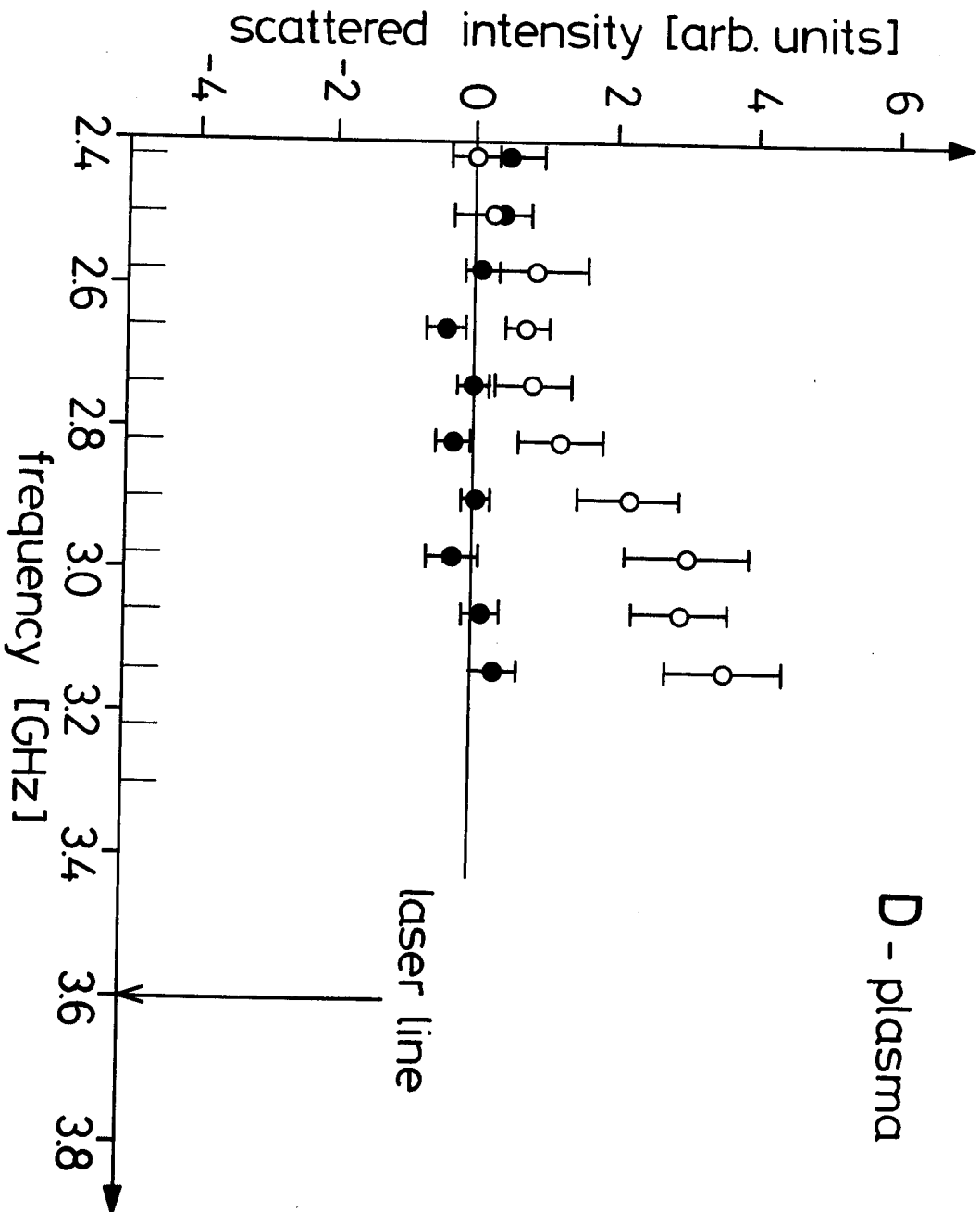
|                   | H-Plasma                          | D-Plasma                          | He-Plasma                         |
|-------------------|-----------------------------------|-----------------------------------|-----------------------------------|
| $N_e$             | $5.5 \cdot 10^{19} \text{m}^{-3}$ | $5.3 \cdot 10^{19} \text{m}^{-3}$ | $5.0 \cdot 10^{19} \text{m}^{-3}$ |
| $T_e$             | 680 eV                            | 830 eV                            | 600 eV                            |
| $Z_{\text{eff}}$  | 2.5                               | 2.5                               | 2.7                               |
| $T_i(\text{fit})$ | 250 eV                            | 310 eV                            | 380 eV                            |
|                   | 320                               | 450                               | 430                               |
|                   | 440                               | 320                               | 370                               |
|                   | 230                               | 460                               | 410                               |
|                   | 260                               | 220                               | 470                               |
|                   | 370                               | 300                               | 260                               |
|                   | 460                               | 480                               | 470                               |
|                   | 300                               | 490                               | 270                               |
|                   | 320                               | 450                               | 400                               |
| mean              | 330 ( $\pm 30$ ) eV               | 390 ( $\pm 30$ ) eV               | 390 ( $\pm 25$ ) eV               |
| stand. dev.       | 80 eV                             | 100 eV                            | 80 eV                             |
| rel. error        | 25%                               | 26%                               | 20%                               |







# D - plasma



# He-plasma

